PCP
PLANT & CELL PHYSIOLOGY

Plasticity of DNA methylation and gene expression under zinc deficiency in Arabidopsis roots

Xiaochao Chen, Brigitte Schönberger, Jochen Menz and Uwe Ludewig*

Institute of Crop Science, Nutritional Crop Physiology, University of Hohenheim, Fruwirthstr. 20, D-70593 Stuttgart, Germany
*Corresponding author: E-mail, u.ludewig@uni-hohenheim.de; Fax, +49 711 459 23295
(Received December 1, 2017; Accepted May 10, 2018)

Regular Paper

DNA methylation is a heritable chromatin modification that maintains chromosome stability, regulates transposon silencing and appears to be involved in gene expression in response to environmental conditions. Environmental stress alters DNA methylation patterns that are correlated with gene expression differences. Here, genome-wide differential DNA methylation was identified upon prolonged zinc (Zn) deficiency, leading to hypo- and hypermethylated chromosomal regions. Preferential CpG methylation changes occurred in gene promoters and gene bodies, but did not overlap with transcriptional start sites. Methylation changes were also prominent in transposable elements. In contrast, non-CpG methylation differences were exclusively found in promoters of protein-coding genes and in transposable elements. Strongly Zn deficiency-induced genes and their promoters were mostly non-methylated, irrespective of Zn supply. Differential DNA methylation in the CpG and CHG, but not in the CHH context, was found close to a few up-regulated Zn deficiency genes. However, the transcriptional Zn deficiency response in roots appeared little correlated with associated DNA methylation changes in promoters or gene bodies. Furthermore, under Zn deficiency, developmental defects were identified in an Arabidopsis mutant lacking non-CpG methylation. The root methylome thus responds specifically to a micronutrient deficiency and is important for efficient Zn utilization at low availability, but the relationship of differential methylation and differentially expressed genes is surprisingly poor.

Keywords: Bisulfite sequencing • Chromatin • Index DNA methylome • Micronutrient • Nutritional deficiency.

Abbreviations: mC, methylated cytosine; CHG/CHH, non-CpG, cytosine followed by nucleotides other than guanine in the DNA sequence; CpG, cytosine followed by guanine in the DNA sequence; DEG, differentially expressed gene; DMR, differentially methylated region; FDR,false discovery rate; PCA,principal component analysis; RdDM, RNA-directed DNA methylation; RT–PCR, reverse transcription–PCR; SAM, S-adenosylmethionine; TE, transposable element; TSS, transcription start site; Zn, zinc.

Introduction

DNA methylation is a heritable epigenetic modification of chromatin in living organisms, which plays essential roles in stabilization of the genome against transposable elements (TEs), regulation of transcription and alternative splicing (Chan et al. 2005, Zilberman et al. 2007, Law and Jacobsen 2010, Lev Maor et al. 2015). The methylation of cytosines in plant DNA occurs in the symmetric contexts CpG and CHG (where H represents A, T or C), and the asymmetric context CHH. The methylation is established and maintained by partially independent pathways (Law and Jacobsen 2010), and is affected by environmental factors (Probst and Mittelsten Scheid 2015, Asensi-Fabado et al. 2017). Symmetric methylation can simply be maintained by copying the methylation mark from the complementary strand in dividing cells during chromosome replication. CpG methylation is maintained by METHYLTRANSFERASE 1 (MET1) in Arabidopsis, while CHG methylation is maintained by CHROMOMETHYLASE 3 (CMT3), which further requires H3K9 methylation. CHH methylation, in contrast, cannot simply be copied from the complementary strand and thus must be set by the de novo methylation machinery, which requires DOMAINS REARRANGED METHYLTRANSFERASE 1 (DRM1) and DRM2, via the RNA-directed DNA methylation (RdDM) pathway.

CpG methylation is enriched at TEs as well as in gene bodies, whereas CHG and CHH methylation predominantly occurs at TEs and is generally more dynamic (Cokus et al. 2008, Lister et al. 2008, Stroud et al. 2013). De novo hypermethylation of non-CpG was set by suboptimal temperature in Arabidopsis or by phosphate starvation in rice, while CpG methylation was relatively little affected (Dubin et al. 2015, Secco et al. 2015). Prolonged phosphate starvation stress not only altered the expression of thousands of genes in rice, but additionally roughly 150 TEs close to highly up-regulated genes were hypermethylated, predominantly in the non-CpG context (Secco et al. 2015). Some additional TEs close to differentially expressed genes (DEGs) were predominantly hypomethylated in the CpG context (Secco et al. 2015). Interestingly, changes in the gene expression induced by phosphate starvation preceded DNA hypermethylation at adjacent TEs and were reversible,

Plant Cell Physiol. 59(9): 1790–1802 (2018) doi:10.1093/pcp/pcy100, Advance Access publication on 25 May 2018, available online at www.pcp.oxfordjournals.org

but not heritable (Secco et al. 2015). This suggested methylation as a transient consequence, rather than the cause of differential gene expression. While the same study reported this mechanism only to be present to a very limited extent in Arabidopsis (Secco et al. 2015), another study showed general correlations of phosphate starvation-regulated gene expression in Arabidopsis with both individual differentially methylated cytosines and differentially methylated regions (DMRs; Yong-Villalobos et al. 2015). In addition to the association of gene activation with hypermethylation of neighboring TEs, they also frequently observed parallel gene activation associated with demethylation in the gene body or in upstream regions (Yong-Villalobos et al. 2015). Furthermore, data from seedlings of different ages showed that DNA methylation changed massively during Arabidopsis development and that methylation mutants had increased sensitivity to phosphate starvation (Yong-Villalobos et al. 2015). A mutant that has massively lost non-CpG methylation, with little effect on CpG methylation, is the triple mutant ddc (lacking DRM1, DRM2 and CMT3) (Cao and Jacobsen 2002, Lister et al. 2008, Stroud et al. 2013), while the ros1 mutant (repressor of silencing1) is impaired in demethylation, leading to global hypermethylation of genomic DNA (Gong et al. 2002, Le et al. 2014). Besides the mentioned studies on phosphate starvation, relatively little is known about nutritional effects on the methylome and the consequences of altered methylation on the nutrient status (Secco et al. 2017). However, limitation of another macroelement, nitrogen, was also shown to alter DNA methylation patterns. The progeny of nitrogen-limited rice plants even showed enhanced tolerance to the same stress, suggesting transgenerational inheritance (Kou et al. 2011).

With this fragmented knowledge of nutritional regulation of the DNA methylome, we were interested in whether the lack of a micronutrient would also specifically affect the methylome. Zinc (Zn) is an essential cofactor in many enzymes and, notably in DNA-binding proteins, such as the large family of Zn-finger transcription factors, has pleiotropic functions in plant metabolism and is crucial for gene expression and protein synthesis (Broadley et al. 2007). Zn deficiency is associated with the differential expression of hundreds of genes in roots and shoots (van de Mortel et al. 2006). We hypothesized that prolonged Zn deficiency would alter the methylome in Arabidopsis roots in a way that correlates well with the transcriptional response to −Zn. Furthermore, we hypothesized that mutants with aberrant DNA methylation might fail to cope properly with nutritional stress, such as −Zn, which might support a role for methylation in the nutritional stress tolerance.

Results

Prolonged mild Zn deficiency and transcriptional profiling of Sf-2 Arabidopsis thaliana roots

A previous microarray analysis had identified >300 differentially expressed transcripts in shoots and roots of the Arabidopsis Col-0 accession in response to the absence of (0 μM) and high (25 μM) Zn (van de Mortel et al. 2006). Because severe −Zn stress induces developmental phenotypes and alters flowering, we first established hydroponic growth conditions in which the root and shoot development in +Zn and −Zn was similar, to capture plants in the same developmental stages for subsequent mRNA extraction and microarray analysis. In our previous analysis of many A. thaliana genotypes that used and translocated Zn differentially to the seed (Chen et al. 2016), we had identified the late flowering and large biomass-producing Sf-2 as a genotype that robustly grows similar roots and shoots under +Zn and −Zn. This accession was initially little affected by the −Zn treatment, thus had an efficient −Zn response and was therefore selected for subsequent analysis. Sf-2 plants were harvested 40 d after sowing and the ionome of the shoot confirmed the Zn deficiency (+Zn, 72.8 μg g^{-1} and −Zn, 11.1 μg g^{-1}) (**Fig. 1A, B**). All other nutrients were in the sufficiency range, although copper (Cu) was also reduced and calcium (Ca) slightly elevated in the −Zn treatment. Nevertheless, the biomass was not reduced under −Zn (**Fig. 1C**), suggesting that this genotype was 'Zn efficient'. Visual symptoms of Zn deficiency, such as gray necrotic spots in the apical zone of mature leaves, were observed at later stages, but no signs of the initiation of flowering were apparent after 6 weeks (**Fig. 1D**).

The microarray analysis was conducted in triplicate and identified 189 and 430 genes that were >2-fold up- and down-regulated under prolonged −Zn, respectively, but roughly 20% of the up-regulated transcripts were non-protein coding (Supplementary Table S1). Similar microarray analysis after transfer to 0 μM Zn in the accession Col-0 had identified 221 and 78 protein-coding genes that were at least 2-fold up- or down-regulated, respectively (van de Mortel et al. 2006). To our surprise, only 18% of these differentially regulated protein-coding genes overlapped between Sf-2 and Col-0. Using more strict significance thresholds and corrections for large data sets to obtain a false discovery rate (FDR) of $P < 0.05$, only 14 DEGs with −Zn remained in Sf-2 (**Table 1**; Supplementary Table S1). This core set of −Zn-induced genes included the Zn transporter family genes, ZIP1, ZIP3, ZIP4, ZIP5 and IRT3, as well as the nicotinamine synthase genes NAS2 and NAS4. Furthermore, the heavy metal ATPase gene HMA2 and the purple acid phosphatase gene PAP27 were strongly up-regulated. All these genes were confirmed by quantitative reverse transcription–PCR (qRT–PCR) (**Fig. 1E**) and had also been identified in Col-0 (van de Mortel et al. 2006). These genes thus represent the core set of −Zn deficiency-induced genes across different Arabidopsis accessions. Interestingly, four genes encoding defensin-like family proteins were most highly up-regulated by −Zn, which had not come to attention in the accession Col-0. The only down-regulated transcript in this list of the most stringent regulated genes in −Zn was TERMINAL FLOWERING 1 (TFL1), a gene involved in flowering (**Fig. 1E**).

A principal component analysis (PCA) of the gene expression profiles identified that the majority of the variance within the data (60.3%) was unrelated to the Zn deficiency and represented other factors, while the second principal component,

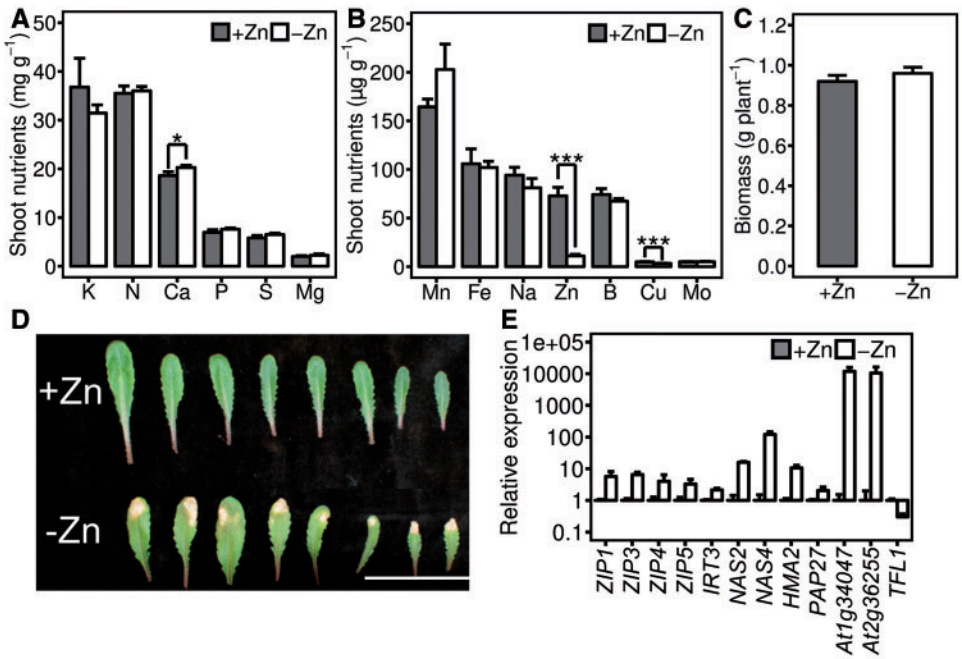

Fig. 1 Zn deficiency in the accession Sf-2. (A, B) Mineral concentrations of +Zn and −Zn in shoots. Data are plotted as mean ± SD. * and *** indicate significant differences at the $P < 0.05$ and $P < 0.001$ level, respectively. (C) Dry shoot biomass in full nutrition (+Zn, 2 μM $ZnSO_4$) and Zn deficiency (−Zn) at 40 d. (D) Visible Zn deficiency symptoms in Arabidopsis leaves at 40 d. Necrosis appeared in young leaves. Scale bar = 5 cm. (E) Verification of differentially expressed transcripts identified in microarray by qRT–PCR. Reference genes *PDF2* and *SAND* were used for normalization, relative to +Zn.

Table 1 Differentially expressed transcripts identified by microarray, log fold changes, adjusted *P*-value and mean expression intensity

Number	Name	AGI code	Annotation	Log_2FC	Adjusted *P*-value	Mean intensity	CpG (%)		CHG (%)		CHH (%)	
							+Zn	−Zn	+Zn	−Zn	+Zn	−Zn
1	*ZIP1*	*AT3G12750.1*	Zinc transporter 1	2.18	0.018	5257	3.0	3.1	0.3	0.4	0.3	0.5
2	*ZIP3*	*AT2G32270.1*	Zinc transporter 3	2.41	0.005	6747	0.4	0.5	0.6	0.5	0.3	0.4
3	*ZIP4*	*AT1G10970.1*	Zinc transporter 4	2.67	0.015	3616	17.9	15.5	0.8	1.0	0.4	0.4
4	*ZIP5*	*AT1G05300.1*	Zinc transporter 5	2.80	0.021	1965	0.2	0.3	0.2	0.2	0.3	0.3
5	*ZIP5*	*AT1G05300.2*	Zinc transporter 5	2.25	0.015	36	0.2	0.3	0.2	0.2	0.3	0.3
6	*IRT3*	*AT1G60960.1*	Iron regulated transporter 3	2.15	0.007	6562	6.2	5.6	0.4	0.2	0.3	0.3
7	*NAS2*	*AT5G56080.1*	Nicotianamine synthase 2	4.49	0.012	186	1.1	0.6	0.7	0.2	0.3	0.3
8	*NAS4*	*AT1G56430.1*	Nicotianamine synthase 4	5.62	0.023	71	6.2	2.4	2.3	0.2	1.0	0.4
9	*HMA2*	*AT4G30110.1*	Heavy metal atpase 2	4.43	0.026	495	6.4	6.5	0.3	0.4	0.3	0.3
10	*PAP27*	*AT5G50400.1*	Purple acid phosphatase 27	2.01	0.025	1911	12.7	10.3	0.4	0.3	0.4	0.3
11	*DEFL*	*AT1G34047.2*	Defensin-like family protein	10.49	0.008	530	0.6	0.6	0.3	0.4	0.3	0.6
12	*DEFL*	*AT2G36255.1*	Defensin-like family protein	10.60	0.012	313	0.2	0.3	0.0	0.0	0.5	0.5
13	*DEFL*	*AT3G59930.1*	Defensin-like family protein	8.71	0.036	512	2.5	0.3	2.0	0.2	1.1	0.5
14	*DEFL*	*AT4G11393.1*	Defensin-like family protein	8.50	0.012	372	0.0	0.1	0.0	0.2	0.0	0.2
15	*TFL1*	*AT5G03840.1*	Terminal flower 1	−1.48	0.025	91	0.1	0.6	0.5	0.3	0.4	0.4

Gene body methylation level in the different contexts is given as a percentage.

which explained 19.3% of the variance, separated the data according to the −Zn and +Zn treatments. This suggests unknown and phenotypically unrecognized variance within the +Zn samples. The samples from the −Zn treatment were more similar to each each other (**Fig. 2A**).

Genome-wide DNA methylation profiling of Arabidopsis roots upon Zn deficiency

Since nutrient stress was reported to drive hypermethylation in TEs close to highly regulated genes, we hypothesized that

the methylome of −Zn roots is affected by the prolonged Zn deficiency. The DNA methylome profile at single-base resolution in Sf-2 Arabidopsis under +Zn and −Zn was then measured with whole-genome bisulfite sequencing on the same pooled root samples that had been used for the microarray analysis, each in triplicate. Bisulfite sequencing yielded approximately 40 million clean paired-end reads for each sample (Supplementary Table S2). Altogether, average coverage was 22.3× (7.8–29.9×) and the average unique mapping rate amounted to 32.3% (15.5–41.3%). Bisulfite non-conversion rates were relatively low. Strict alignment settings were used to limit aligning mismatches (see the Materials and Methods for details). Nevertheless, relatively low mapping rates that may in part be due to mapping of Sf-2 reads to the imperfectly matching Col-0 genome were obtained (Supplementary Table S2).

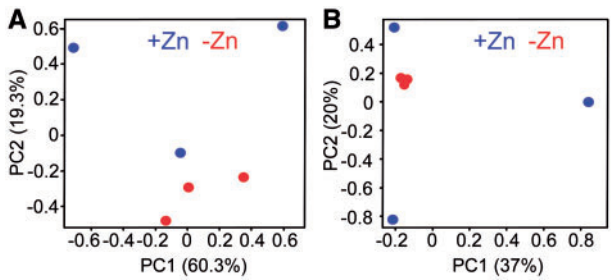

Fig. 2 Principal component (PC) analysis of the microarray data and DNA methylation. (A) Plot of the first two PCs for normalized microarray data containing all genes, explaining 79.6% of the data variance with +Zn (blue) and −Zn (red). (B) Plot of the first two PCs explaining 57% of the variance of the methylation level in total ^{m}Cs under +Zn (blue) and −Zn (red). The different symbols represent the different replicates.

The PCA of the methylation pattern identified large separation of the +Zn samples, while all −Zn samples were found close to each other, consistent with their transcriptional homogeneity (**Fig. 2B**). Among the aligned mCs (methylated cytosines), the whole-genome methylation levels of CpG, CHG and CHH were 22.7, 7.6 and 3.0% in +Zn and similar under −Zn (**Fig. 3A**). The proportion of CpG, CHG and CHH of total cytosine methylation amounted to 53.4, 18.0 and 28.6% for +Zn and 54.0, 16.7 and 29.3% for −Zn, respectively (**Fig. 3B**). Because certain small RNA fractions were repressed in DNA methylation mutants (Lister et al. 2008), the small RNA level was also estimated. The total small RNA level was not significantly different, although it was slightly lower under −Zn conditions (**Fig. 3C**). The minor demethylation pattern induced by −Zn may simply be a consequence of low S-adenosylmethionine (SAM), the donor of methyl groups, but the SAM level was more or less maintained under −Zn (Supplementary Fig. S1). Differential methylation mainly occurred in the CpG context and was rare in the CHH context (see below, **Fig. 3D**).

To determine whether genomic DNA methylation in the roots correlates with gene expression, we divided all transcripts into three classes, based on their average expression intensity in the microarray analysis, namely high expression (top third, n = 10,709, average log expression intensity approximately 10.5), medium expression (middle third, n = 10,709, average log expression intensity approximately 6.8) and low expression (bottom third, n = 10,710, average log expression intensity approximately 3.0). Non-methylated regions were excluded before calculating the average methylation level in different groups, as these regions diluted the methylation level across genes. In general, the methylation level of gene bodies in the CpG context was much higher than in the non-CpG context (**Fig. 3E–G**). The methylation level of the genes was slightly reduced, irrespective of the transcript abundance in −Zn,

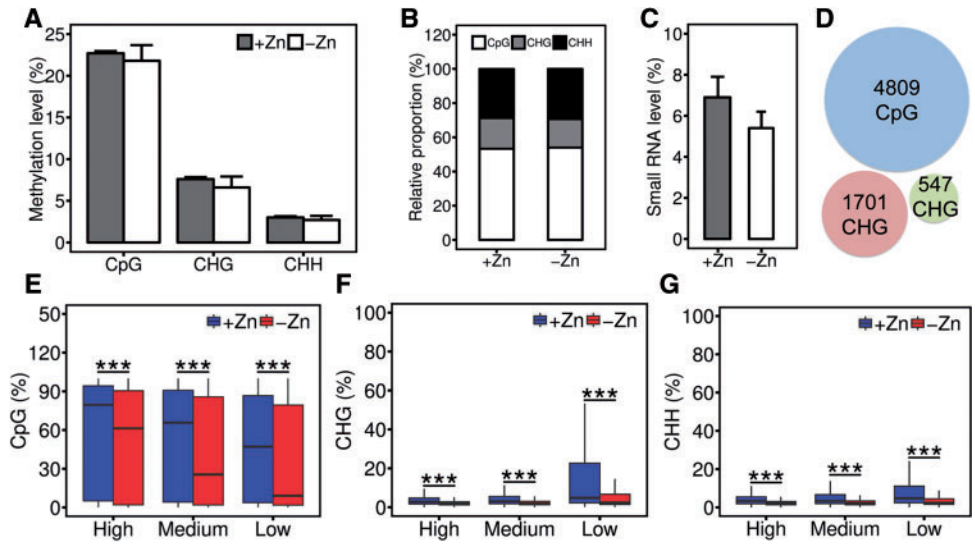

Fig. 3 Methylation level under different Zn supply. (A) Methylation level in the CpG, CHG and CHH context under +Zn and −Zn. (B) Relative proportion of methylation in the genome. (C) Fraction of small RNAs relative to total RNAs. (D) Number of differentially methylated regions in each context. (E–G) Gene body methylation level in different expressed gene groups (high, medium and low expression, see text) in the whole genome. Box plot data with means; *** indicates significant methylation differences at the $P < 0.001$ level between +Zn and −Zn.

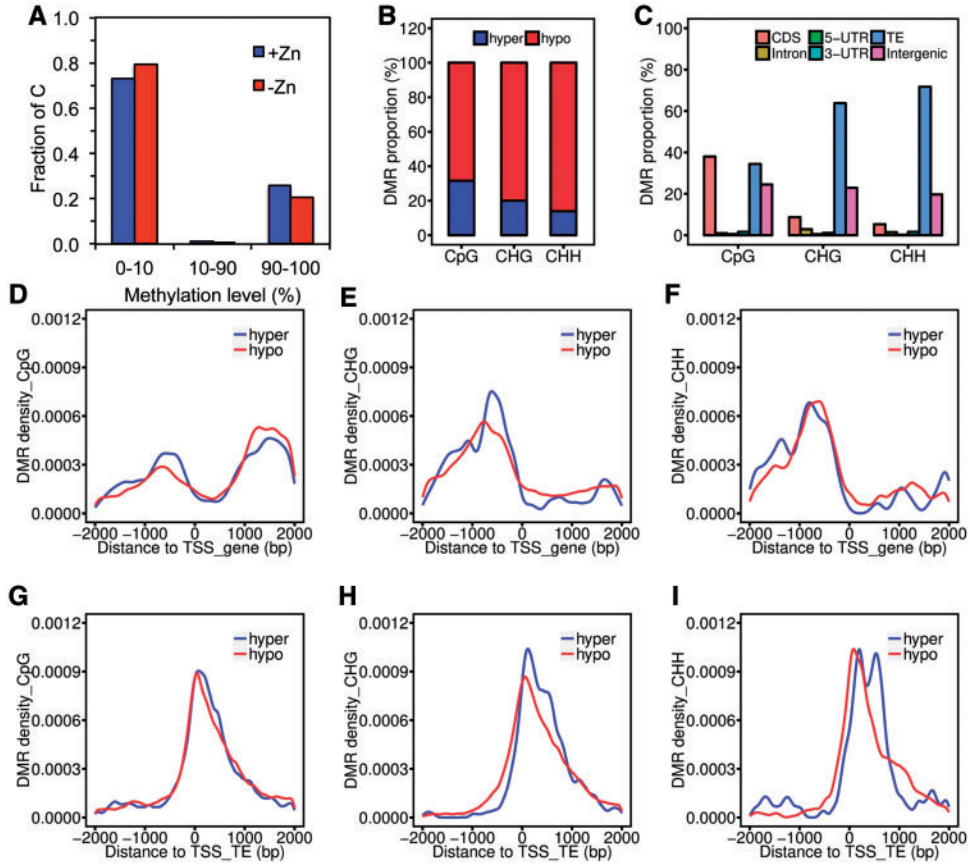

Fig. 4 Distribution of differentially methylated regions (DMRs) in different genomic features and description of DMR distribution across genes and TEs. (A) Fraction of methylated cytosines found at different methylation levels. (B) Relative DMR amounts in different contexts. (C) DMR proportion in different genomic features. (D–F) Normalized DMR distribution around transcription start sites (TSS) of genes. (G–I) Normalized DMR distribution around transposon start site (TSS_TE) of TEs. Hyper (blue) and hypo (red) indicate hypermethylation and hypomethylation in −Zn relative to the +Zn treatment, respectively. Normalization was either to total hypo- or total hypermethylated counts.

while gene expression was always highly correlated with gene body methylation (**Fig. 3E–G**). A slightly higher CpG methylation was detected in the gene bodies of highly expressed genes in +Zn, whereas non-CpG methylation was preferentially found in genes expressed at a low level. The methylation levels of individual cytosines were typically either low (0–10%) or high (90–100%) in the gene bodies, indicating homogeneity within samples, irrespective of the different contexts and irrespective of Zn supply (Supplementary Fig. S2A–F). In −Zn, however, there was a tendency for fewer highly methylated cytosines, but an enrichment of low methylated cytosines (**Fig. 4A**). This was observed in each cytosine context (Supplementary Fig. S2A–C).

Differentially methylated regions induced by Zn deficiency

Although the global methylation amount in all contexts (CpG, CHG and CHH) was little different in −Zn, we noted hundreds of DMRs in −Zn. DMRs define regions in the genome where multiple adjacent cytosines show differential methylation, but it is unknown how many cytosines there are in a certain region and to what extent these must be differentially methylated to have a functional impact. Therefore, a low threshold for methylation differences (10%; see the Materials and Methods) was set, to avoid missing DMRs. Both hypo- and hypermethylated genome regions were identified, but hypomethylated regions dominated the DMRs, especially in the non-CpG context (**Fig. 4 B**). For the analysis of DMRs, methylation calls with ≥2-fold coverage in at least two replicates were included. Thereby, 4,809 DMRs in CpG, 1,701 DMRs in CHG and 547 DMRs in CHH were determined (**Fig. 3D**). DMRs in the CpG context were mainly located in the gene bodies, TEs and intergenic regions, whereas DMRs in the non-CpG contexts occurred predominantly in TEs, but also in intergenic regions (**Fig. 4C**).

The DMR density across the protein-coding genes was analyzed in a 4 kb window that was centered in the transcriptional start site (TSS). This captured the promoter region up to 2 kb upstream of the TSS and at least part of the gene body (**Fig. 4D–F**). Although hypomethylation was more frequent in each context (**Fig. 4B**), the pattern of DMRs around the TSS was highly similar. When normalized to the total numbers of hypomethylated DMRs, most CpG hypo-DMRs in the promoter peaked at around 700 bp upstream of the TSS, but this peak was at approximately 1,400 bp downstream of the TSS,

covering the gene bodies (Fig. 4D). A very similar pattern within the 4 kb window around the TSS was obtained for the hypermethylated DMRs (Fig. 4 D). Similar to previous studies, cytosines in the gene TSS were always very rarely methylated. Interestingly, both hypo- and hypermethylation in the CHG and CHH context occurred again predominantly in promoters with a peak at around 700 bp upstream from the TSS (Fig. 4E, F). However, in the non-CpG context, no DMRs were identified in the gene bodies. DMRs were even more prominent in TEs and overlapped with the transposon start sites in all contexts (Fig. 4G–I). Again, these were either hypo- or hypermethylated in −Zn. Besides these regular patterns, stochastic DMRs were also identified in individual samples with the same treatment, showing considerable intrinsic variation among the equally treated individual samples, in agreement with the PCA results (Fig. 2 B).

Relationship of gene expression and DNA methylation in −Zn

Next we asked whether methylation and/or differential methylation occurred in or close to the 14 genes that were transcribed highly differently in −Zn (Table 1; Supplementary Table S1). The gene bodies of these DEGs were rarely methylated in all contexts (Table 1). However, despite their low methylation level, the methylation of NAS2, NAS4 and one defensin-like gene (At3g59930) was apparently slightly different. Methylation was reduced in −Zn in the CpG and CHG context. In most DEGs that were close to DMRs, hypomethylation was encountered in −Zn, but the majority of genes were very distant from DMRs. Only one of the associated gene bodies partially overlapped with a DMR (Table 2). In particular, all DMRs in the CHH context were very distant from these DEGs. Within the distance of 2.5 kb, hypo-DMRs upstream of ZIP1 and ZIP3 and downstream of IRT3 and NAS2 were detected. DMRs upstream and in the gene body of PAP27 were also detected. DMRs were also close to the defensin-like-encoding DEFL genes At4G11393 and At1G34047.

Next we selected all genes that were covered by DMRs in the gene body and in 2 kb upstream sequences. Furthermore, we also selected genes that were 2 kb distant from TEs, which were covered by DMRs. For these genes, −Zn-induced alterations in methylation and transcriptional differences (without considering significance thresholds) were directly compared. Surprisingly, there was clearly a lack of any global correlation between differential methylation and mRNA abundance, irrespective of the mC contexts (Fig. 5). Gene body methylation changes (Fig. 5A–C), as well as methylation differences in promoters (Fig. 5D–F), were only rarely associated with altered transcript levels. Overall, the majority of responsive genes were unchanged in their methylation pattern. Moreover, this same pattern was also found for TEs (Fig. 5G–I) and in the entire genome (Supplementary Fig. S3).

Single-cytosine methylation in the Zn deficiency-responsive motif

We finally analyzed the single-cytosine methylation in the previously identified Zn deficiency-responsive motif (RTGTCGAC AY) in promoters that is targeted by transcription factor genes bZIP19 (BASIC-REGION LEUCINE ZIPPER 19) and bZIP23 in response to −Zn (Assuncao et al. 2010). This 10 bp motif contains two consensus cytosines, which are in the CpG and CHH context, respectively. By alignment to TAIR10, we found 83 genes that contain this motif in their promoters without mismatch, including ZIP4, ZIP5, IRT3 and two defensin-like genes (AT1G34047 and AT4G11393), which were also identified in the microarray analysis (Supplementary Table S3). The other −Zn-induced genes often contained similar motifs with minor mismatches. Only 58 of the 83 gene promoters overlapped with the methylome data, but the methylation level of both cytosines was consistently low across all these genes. Only very minor

Table 2 Closest DMRs to the differentially expressed genes

Transcripts			Closest DMR_CpGs			Closest DMR_CHGs			Closest DMR_CHHs		
Number	Name	AGI code	Type	Location	Distance (bp)	Type	Location	Distance (bp)	Type	Location	Distance (bp)
1	*ZIP1*	*AT3G12750.1*	**Hypo**	**Upstream**	**1413**	Hyper	Downstream	112111	Hypo	Downstream	65491
2	*ZIP3*	*AT2G32270.1*	**Hypo**	**Upstream**	**1612**	**Hypo**	**Upstream**	**1367**	Hypo	Downstream	69565
3	*ZIP4*	*AT1G10970.1*	Hypo	Downstream	8035	Hypo	Downstream	117338	Hyper	Downstream	159313
4 + 5	*ZIP5*	*AT1G05300*	Hypo	Downstream	22332	Hypo	Downstream	99594	Hypo	Upstream	22212
6	*IRT3*	*AT1G60960.1*	**Hypo**	**Downstream**	**1950**	Hyper	Downstream	27221	Hypo	Downstream	145289
7	*NAS2*	*AT5G56080.1*	**Hypo**	**Downstream**	**2452**	Hypo	Downstream	35942	Hypo	Downstream	198989
8	*NAS4*	*AT1G56430.1*	Hypo	Downstream	6882	Hyper	Upstream	8086	Hypo	Upstream	52813
9	*HMA2*	*AT4G30110.1*	Hypo	Upstream	46524	Hypo	Upstream	88708	Hypo	Upstream	459915
10	*PAP27*	*AT5G50400.1*	**Hypo**	**gene body**	**1217**	**Hypo**	**Upstream**	**1187**	Hypo	Downstream	113440
11	*DEFL*	*AT1G34047.2*	**Hyper**	**Upstream**	**190**	**Hypo**	**Upstream**	**557**	Hypo	Upstream	53258
12	*DEFL*	*AT2G36255.1*	Hypo	Downstream	10721	Hypo	Downstream	66379	Hyper	Upstream	67029
13	*DEFL*	*AT3G59930.1*	Hypo	Downstream	18844	Hypo	Downstream	18792	Hypo	Upstream	19932
14	*DEFL*	*AT4G11393.1*	Hyper	Downstream	20906	**Hyper**	**Downstream**	**2246**	Hypo	Downstream	86277
15	*TFL1*	*AT5G03840.1*	Hyper	Downstream	52498	Hypo	Downstream	148868	Hypo	Upstream	317983

Genes in bold are within 2.5 kb distance of the next DMR.

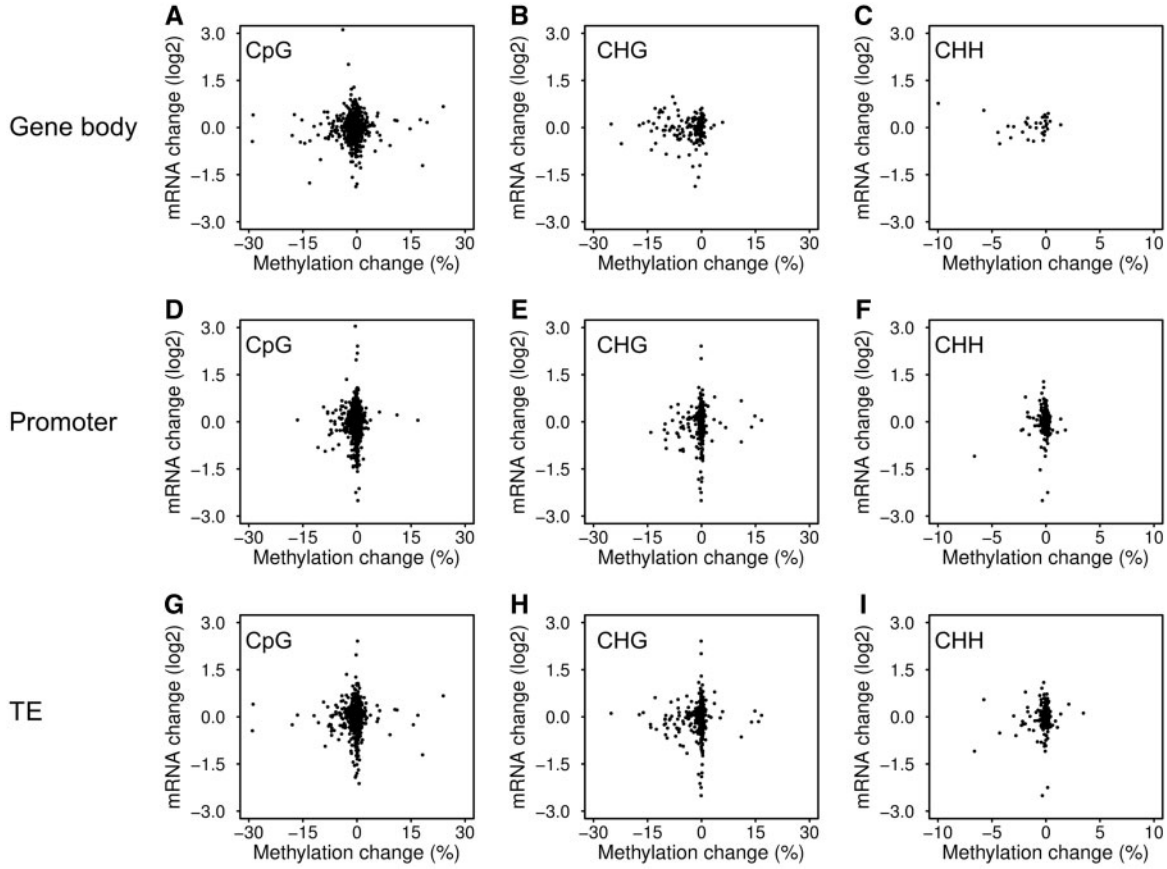

Fig. 5 Lack of correlation between gene transcription and differential DNA methylated regions. (A–C) Gene body methylation. (D–F) Promoter methylation. The promoters were defined as sequences 2 kb upstream of the transcription start site (TSS). (G–I) Transposable element (TE) methylation. Only TEs that either overlapped with gene bodies or were located up to 2 kb upstream of the gene TSSs were chosen. Non-methylated genes and transposons were omitted.

differences in methylation of a subset of the genes were found (Supplementary Table S4), indicating that −Zn had little effect on the methylation level in individual cytosines in this −Zn motif. Overall, there was essentially a lack of any clear correlation between differential methylation in the motif and gene expression changes upon −Zn.

Growth of methylation mutants under Zn deficiency

The ddc triple mutant (drm1, drm2, cmt3) that has massively reduced non-CpG methylation was then grown side by side with the Col-0 wild type in hydroponic culture under long-day conditions. Consistent with earlier work, the mutant showed mild developmental phenotypes, but reduced overall growth. When Zn was selectively omitted from the nutrient solution, the Col-0 wild type and the ddc mutant accumulated only about half of the shoot biomass (**Fig. 6A, B**). In order to test whether the ddc mutant was less efficiently accumulating Zn, the shoot Zn concentrations were measured. The wild type and the ddc mutant accumulated $>44\,\mu g$ Zn g^{-1} DW in the shoot tissue under +Zn. The shoot Zn concentrations of both genotypes were significantly lower in −Zn, but still above the tentative starvation threshold of Arabidopsis at approximately 15–20 $\mu g\ g^{-1}$ (**Fig. 6C**). Although not significant, the mutant tended to have even higher Zn concentrations in the shoot under −Zn than the wild type, potentially indicating that the severe Zn deficiency phenotype of the ddc mutant was not related to less efficient Zn uptake, but rather less efficient utilization of tissue Zn, a phenomenon well known as differential Zn efficiency (Cakmak et al. 1998). Furthermore, the shoot biomass of the hypermethylated ros1 mutant was more severely reduced under −Zn than the wild type, which was paralleled by a decrease in the Zn shoot concentration under −Zn (**Fig. 6A–C**). This observation is in agreement with the hypothesis that in the hypermethylated mutant Zn uptake under −Zn was impaired; the reduced tissue Zn was then likely to be insufficient for shoot growth.

Interestingly, severe developmental differences, a bushy growth, smaller leaves, together with shorter stems and impaired flower development were consistently observed in the ddc mutant under −Zn (**Fig. 6D**). These visible shoot phenotypes resembled the severe Zn deficiency symptoms observed earlier in the Col-0 wild type (Talukdar and Aarts 2008). Moreover, the root biomass was not different when grown with or without Zn in the wild type and ros1 (**Fig. 6 E**). In contrast, the ddc mutant had similar root biomass to the

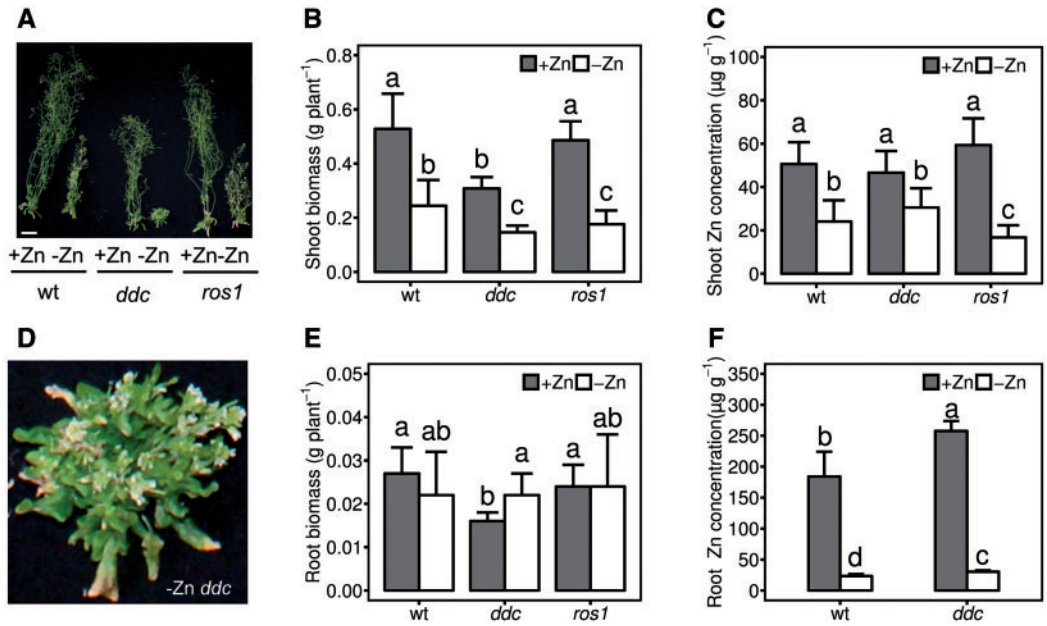

Fig. 6 Arabidopsis methylation mutants under +Zn and −Zn. (A) Phenotypes of the wild type (Col-0), *ddc* mutant and *ros1* mutant under +Zn (2 µM $ZnSO_4$) and −Zn grown in long-day conditions. Scale bar = 5 cm. Shoot dry biomass (B) and Zn concentrations (C) of the wild type and mutants. (D) Phenotype of a −Zn *ddc* mutant plant. Root biomass (E) and root Zn concentrations (F). Data plotted are the mean ± SD. Different letters indicate a significant difference at the $P < 0.05$ level.

wild type and ros1 under −Zn, but less root biomass with +Zn (**Fig. 6 E**). Finally, the Zn concentration in ddc roots was slightly, but significantly, larger than in the wild type, under both +Zn and −Zn, corroborating the suggestion that this mutant was not primarily impaired in the uptake of Zn, but rather in its utilization to produce biomass and transfer Zn to the shoot (**Fig. 6 F**). Altogether, these data show that mutants with altered DNA methylation levels are differentially affected under −Zn conditions, suggesting that the DNA methylation level is important under this stress, to maintain growth in −Zn.

Discussion

DNA methylation is affected by adverse environmental conditions, silences transposons and regulates gene expression. Biotic stress adaptation has been repeatedly associated with chromatin changes, especially of altered DNA methylation (Dowen et al. 2012, Latzel et al. 2012), but relatively little is known about how nutritional deficiencies, which are crucial and widespread abiotic stresses for plants, affect the methylome (Secco et al. 2017).

Zn is an essential micronutrient and cofactor of many DNA-binding transcription factors and enzymes that are involved in vital molecular and metabolic functions (Broadley et al. 2007). Whether and how the Zn status interacts with DNA methylation was comprehensively analyzed by measuring gene transcription and parallel global DNA methylation in the root, the organ that is central for uptake and distribution of nutrients. Prolonged Zn deficiency in a genotype that is little affected in its development by the missing Zn was chosen to capture long-term changes in the absence of secondary developmental effects. We were able to establish such conditions for the A. thaliana accession Sf-2, which is late flowering and able to produce a higher biomass than Col-0. After 6 weeks, visible −Zn-induced necrosis appeared in leaves, without changing the biomass (**Fig. 1**). The ionome indicated specific Zn deficiency in the shoot, and the transcriptomic analysis identified a core set of 14 highly Zn-specific, mostly up-regulated genes that are also found in Col-0. TFL1, a repressor of flowering, was identified to be down-regulated in −Zn, which might indicate a somewhat distinct developmental stage of the plants and roots, potentially explaining some of the heterogeneity in the data of relatively old plants, although they were visually similar. Interestingly, the PCA indicated that much of the variance within the transcriptome data was buried within the +Zn data, while the −Zn transcriptome data were less heterogenous (**Fig. 2A**). Bisulfite sequencing of the roots revealed a large divergence of the variance among individual +Zn samples, but high similarity of the −Zn samples (**Fig. 2B**), suggesting higher heterogeneity in the +Zn plants after the prolonged growth. This also strongly suggests many stochastic mC differences in the +Zn samples. Our analysis indicated a minor overall decrease in methylation level, as well as lower methylation in gene bodies in −Zn, which was most pronounced in genes expressed at a low level in the non-CpG context (**Fig. 3**). Furthermore, context-specific hypo- and hypermethylation in TEs and close to genes were encountered (**Fig. 4**). Because of the minor demethylation trend in −Zn, we also investigated whether the methyl donors were reduced in −Zn. Lower SAM in msa1 strongly reduced the DNA methylation landscape and increased shoot sulfur (Huang et al. 2016). In rats, the SAM level

was decreased under Zn deficiency, therefore DNA and histones were both hypomethylated under −Zn stress (Sharif et al. 2012). However, the Arabidopsis SAM level was not significantly reduced in −Zn (Supplementary Fig. S1), excluding the possibility that a lack of methyl donors was causal for the (minor) reduction in methylation. Furthermore, the major genes involved in the maintenance of CpG and CHG methylation, MET1 and CMT3, respectively, were transcriptionally not affected by Zn, as deduced from the microarray data (Supplementary Table S1).

To date, relatively few studies have investigated the whole-genome DNA methylation profile upon nutrient deficiency, and its potential to regulate transcription (Secco et al. 2015, Yong-Villalobos et al. 2015, Huang et al. 2016). Phosphate starvation-induced gene expression drove DNA hypermethylation at adjacent TEs to stabilize the genome in rice, and the same stress in Arabidopsis conferred massive remodeling of DNA methylation (Secco et al. et al. 2015, Yong-Villalobos et al. 2015). Here, −Zn-induced DMRs in the CpG, CHG and CHH context were identified (**Fig. 4**), in addition to minor intrinsic stochastic differences between individual samples (Dubin et al. 2015). Zn deficiency-related DMRs were not only enriched in TEs in non-CpG contexts, but also occurred in exons and promoters (**Fig. 4**). Both hypo- and hypermethylation DMRs were identified in DEGs, but only in the CpG and CHG context. Clearly, the previously shown nutrient starvation-induced DNA hypermethylation of transposons primarily in the CHH context that is associated with altered gene expression (Secco et al. 2015, Yong-Villalobos et al. 2015) was entirely absent in Zn-deficient Arabidopsis roots. De novo CHH methylation may be the most flexible context to adapt to biotic (Dowen et al. 2012) or other abiotic environmental stress (Dubin et al. 2015, Secco et al. 2015, Yong-Villalobos et al. 2015), but CHH methylation did not respond much to Zn deficiency and was not associated with DEGs. Species differences and nutrient specificity may account for the differences in methylation pattern upon different stresses. −Zn mildly erased and established new DNA methylation in promoters and in gene bodies only in the CpG context, while DMRs in the CHG and CHH context were exclusively set in promoters, with the maxima around 700 bp upstream from the TSS, which may indicate spatial constraints to set and remove DNA methylation with proteins on the DNA strands. An even stronger change with −Zn was found in the methylation of TEs, without preference for hypo- or hypermethylation in all contexts (**Fig. 4**). However, this flexibility in methylation was apparently not mirrored in differential −Zn-induced global gene expression. This was surprising, as DNA methylation plays crucial roles in regulating transcription and alternative splicing (Chan et al. 2005, Zilberman et al. 2007, Law and Jacobsen 2010, Lev Maor et al. 2015). Indeed, taking the 14 highly significantly differentially expressed genes upon −Zn in the accession Sf-2, all were methylated at a very low level (if at all, **Table 1**). These genes include the important Zn deficiency-responsive genes ZIP1, ZIP3, ZIP4, ZIP5, IRT3, NAS2, NAS4, HMA2 and PAP27, which have been characterized in mobilizing Zn or increasing uptake and transfer of Zn (Grotz et al. 1998, van de Mortel et al. 2006, Kramer et al. 2007, Lin et al. 2009). Environmentally responsive genes typically have low methylation in their gene bodies (Aceituno et al. 2008). Furthermore, several genes encoding defensin-like proteins were among the most differentially regulated genes; these were previously not found to be transcriptionally up-regulated by −Zn. However, defensin-like proteins had been identified in the Zn deficiency response proteome and may have a function in capturing or chelating Zn (Zargar et al. 2015). Previous microarray analyses had identified >300 differentially expressed transcripts in response to −Zn in Col-0 (van de Mortel et al. 2006), but this may simply be a consequence of different growth conditions, developmental stage and analysis. Using less stringent quality parameters, another 51 transcripts, including additional Zn transporters and carbonic anhydrases, also appeared differentially expressed in our data set between +Zn and −Zn from Sf-2 (Supplementary Table S1). This set of DEGs largely overlapped with data from the previous study.

Overall, there was almost a lack of global correlation between methylation and gene expression (**Fig. 5**), but it is notable that half of the stringent DEGs had DMRs in the CpG and/or CHG context in their vicinity that were preferentially hypomethylated in −Zn. Considering the large number of 33,601 nuclear-encoded genes (including pseudogenes and TEs, TAIR10) and the 7,057 DMRs identified here, such enrichment is very unlikely by chance. Assuming that gene body methylation is a consequence of transcription rather than the cause (Teixeira and Colot 2009, Inagaki and Kakutani 2012, Secco et al. 2015), any nutrient deficiency-related gene expression will thus lead to an altered methylation profile, which is, however, still difficult to predict.

Finally, we analyzed the single-cytosine methylation in the several dozens of genes that contained the Zn deficiency motif (RTGTCGACAY) in promoters. Most of the stringent DEGs contained this exact motif, but some also had single base pair mismatches, as previously reported (Assuncao et al. 2010). Cytosine methylation in transcription factor-binding sites may alter the binding strength of a vast variety of transcription factors (O'Malley et al. 2016). Indeed, sulfur-responsive elements (SUREs) in the promoters of sulfur transporters were hypomethylated in a sulfur-accumulating mutant that had lower levels of SAM, the methyl donor for DNA methylation. Consequently, sulfate uptake transporter genes were overexpressed in roots, explaining the sulfur accumulation phenotype (Huang et al. 2016). Furthermore, the methylation level in the vicinity of P starvation involved transcription factor-binding sites correlated with differential expression of P starvation-induced genes (Yong-Villalobos et al. 2016). However, the (low) methylation level of most of these cytosines was not distinguishable between the two Zn treatments (Supplementary Table S4), with the exception of three genes (NAS2, NAS4 and DEFL) that had very minor differences in methylation. It might be interesting to test whether this promoter motif could be inactivated by methylation in a tissue that is not or is less sensitive to Zn deficiency.

Early generations of the ddc hypomethylation and ros1 hypermethylation mutants allow for testing the impact of genome-wide differential methylation under nutritional

stresses, as initial generations of these mutants are phenotypically relatively weakly affected in their growth. However, these have severe defects and variable offspring in later generations (Cao and Jacobsen 2002, Gong et al. 2002). Interestingly, the loss of demethylation capacity in ros1 mutants was apparent in initial screens for abiotic stress resistance and the lost ability to repress the RD29A promoter by silencing (Gong et al. 2002).

In contrast to biotic stress (Dowen et al. 2012), where Arabidopsis DNA methylation mutants had increased biotic tolerance, plants lacking non-CpG methylation (ddc triple mutant) were hypersensitive to −Zn (**Fig. 6**), suggesting that methylation is important for the stress tolerance. This hypomethylated mutant showed an interesting developmental phenotype in −Zn, with aberrant leaf and flower development, which was not observed in the wild type (**Fig. 6**). The same phenotype had been described as typical for severe Zn deficiency (Talukdar and Aarts 2008), but the shoot Zn concentration of the mutant was not decreased compared with the wild type. Previous studies reported that the SUPERMAN gene is silenced by hypermethylation in SUPERMAN epigenetic alleles, resulting in an abnormal flower structure compared with the wild type (Jacobsen and Meyerowitz 1997, Ito et al. 2003). Furthermore, FWA (FLOWERING WAGENINGEN) is a floral repressor; and hypermethylation in the promoter inhibits FWA expression in the wild type, whereas fwa-1 mutants show late flowering due to lack of methylation (Soppe et al. 2000). Methylation in these sites may be involved in the −Zn-dependent shoot phenotype. Furthermore, the root biomass increased compared with control conditions (**Fig. 6**). Minor effects on the root dry mass and Zn concentrations were also observed for the hypermethylated ros1 mutant (**Fig. 6**), suggesting that DNA methylation is somewhat relevant for the −Zn tolerance. It may, however, also be argued that the 'weaker' mutant was simply more sensitive to the stress. In any case, methylation is then important for the stress tolerance. A previous transcriptome analyses identified that several genes encoding zinc-binding proteins and the ZIP11 transporter gene were up-regulated in the ddc mutant (Kurihara et al. 2008), establishing a further link of Zn, methylation and the RdDM pathway. However, the transcriptomes of the ddc mutant were somewhat inconsistent (Zhang et al. 2006, Kurihara et al. 2008), with only approximately 10% overlap (in only 24 genes) in DEGs among these studies.

The overall function of the deficiency-induced differential methylation remains largely unclear, as transgenerational heritability of environmentally altered methylation appears unlikely, because of efficient reset mechanisms (Iwasaki and Paszkowski 2014). An A. thaliana population collected from different locations had only small (<3% environmentally induced) heritable epigenetic variation, over dozens of generations (Hagmann et al. 2015). Differential methylation upon phosphate starvation was essentially erased after meiosis in rice (Secco et al. 2015). Although DNA methylation may be of restricted relevance in the immediate −Zn response of Arabidopsis, we expect that across evolutionary time scales and in TE-rich species, nutritional effects on the methylome might still be an important (epi-)genotypic property.

Conclusion

Our study identified a defined remodeling of the methylome in −Zn and quite severe developmental consequences of −Zn in a mutant lacking non-CpG methylation. Unlike in phosphate starvation in rice or suboptimal temperature stress in Arabidopsis, −Zn only mildly affected total methylation. However, hypo- and hypermethylated genomic regions, predominantly in TEs, promoters and genes in the CpG/CHG context, were identified, preferentially in the vicinity of transcriptionally responsive genes. We conclude that the relationship between nutrient stress-induced transcription and dynamic DNA methylation is highly species and nutrient specific and not constrained to macronutrients.

Materials and Methods

Plant materials, growth conditions and sample collection

The *A. thaliana* accession Sf-2 was used for most experiments. Plants were grown in a hydroponic system in a growth chamber in triplicate, with each sample containing a minimum of four plants. A modified Hoagland's solution was supplied, containing 1 mM NH_4NO_3, 1 mM KH_2PO_4, 0.5 mM $MgSO_4$, 1 mM $CaCl_2$, 0.1 mM Na_2EDTA-Fe, 2 μM $ZnSO_4$, 9 μM $MnSO_4$, 0.32 μM $CuSO_4$, 46 μM H_3BO_3, 0.016 μM Na_2MoO_4 and with or without 2 μM $ZnSO_4$, resulting in +Zn or −Zn conditions. Because of an unidentified contaminating source of Zn, we were not able to reduce the Zn level below 0.05 μM Zn in the −Zn condition, but this may also be seen as an advantage to prevent cells from the most severe starvation that results in cell death. At 40 d, shoot and root samples were separately harvested with liquid nitrogen, before storing at −80 °C for further analysis. The accession Col-0 was used in the mutant experiments. *ddc* and *ros1* mutants were in the Col-0 background. The growth conditions were set as: long days (16 h light/8 h dark), 22°C light/20°C dark, 120–140 μmol m^{-2} s^{-1} and 60% humidity.

Ionome analysis

Harvested samples were dried at 60°C for 5 d before grinding. Around 0.5 g of ground material was digested with 5 ml of 69% HNO_3 and 4 ml of 30% HCl for 1 h. Afterwards, samples were heated at 170°C for 25 min in a microwave, followed by 40 min at 200°C. The extract was measured by ICP-MS (inductively coupled plasma mass spectrometry), to determine concentrations of P, K, Ca, Mg, B, Zn, Cu, Fe, Mn, Mo and Na. Additionally, approximately 5 mg of ground material was used to quantify N and S concentrations using an Elemental Analyzer (HEKAtec GmbH).

Total RNA isolation and transcriptome analysis

Total RNA of 40-day-old root samples was extracted using the innuPREP Plant RNA Kit (Analytik Jena). Each treatment contained three independent biological replicates. All RNA samples were sent to OakLabs (Germany) for transcriptome analysis on single-channel Agilent microarrays. Raw data analysis was performed using Bioconductor's limma package (Ritchie et al. 2015). The microarray raw data were imported in R with the read.maimages function. The median signal intensities were background corrected with the normexp method. The microarrays were quantile normalized so that the value distribution of every microarray was forced to be identical. Probes with low intensities that were not at least 10% higher than the negative control probes were filtered out. The intensities of duplicated probes for the same corresponding genes

were averaged. The resulting *P*-values were adjusted by the Benjamini–Hochberg approach to control the FDR (Benjamini and Hochberg 1995). Genes were considered to be significantly differentially expressed if the FDR was <0.05.

Genomic DNA extraction and bisulfite sequencing

Genomic DNA of 40-day-old root samples was extracted using the DNeasy Plant Mini Kit (Qiagen) in triplicate for each treatment. DNA samples were sent to Beijing Genomics Institute (BGI, China) for whole-genome bisulfite sequencing. Briefly, the MethylC-Seq library was constructed and sequenced with 100 bp paired-ends, using Illumina Hiseq2000.

DNA methylation data processing

Raw data were filtered to remove the low-quality reads, comprising three types: adaptor sequences, N base number >10% and number of low-quality bases (<20) over 10%. Clean data were mapped to the TAIR10 reference genome (The Arabidopsis Information Resource, http://www.arabidopsis.org/), using Bismark (Krueger and Andrews 2011). Default settings were used, except that the score_min was set as L, 0,-0.6, before removing PCR duplicates with SAMtools (Li et al. 2009). Bismark_methylation_extractor was conducted to call the cytosine methylation in CpG, CHG and CHH contexts. Then 5 and 3 bp bias bases were removed from the 5′ and 3′ end, respectively, according to the M-bias plots produced by the Bismark methylation extractor.

DMR calling was performed using BSmooth in Bioconductor's bsseq package with default settings (Hansen et al. 2012). Briefly, bedGraph output files were smoothed, before computing *t*-statistics. Only those CpGs/CHGs/CHHs where kept that in at least two replicates in each treatment had at least a 2-fold coverage. Then dmrFinder was used to find DMRs. Those DMRs which did not cover at least three CpGs/CHGs/CHHs or showed a mean difference <0.1 were filtered out. This low threshold for DMR detection was chosen in order not to miss any potential DMRs. The qcutoff and maxGap were set as 0.025 and 300 bp.

DMRs were mapped to genomic elements using TAIR10 annotations. Positions and regions were hierarchically assigned to annotated features in the order coding sequence (CDS) > intron > 5-untranslated region (UTR) > 3-UTR > TE > intergenic region. Intergenic regions were defined as those that were annotated with neither gene bodies nor TEs. The mapping was performed using bedtools (Quinlan and Hall 2010). Upstream sequences (2 kb) of gene bodies were also overlapped with DMRs to indicate promoter regions.

The relative DMR density in a 4 kb sliding window across the genome (−2 kb < TSS < 2 kb) was calculated as: DMR density = (hyper- or hypo-) DMR counts at a specific position/total (hyper- or hypo-) counts.

Principal components analysis (PCA)

Normalized intensity data of all microarray experiments and all methylation bins in each context were used. The R-script with prcomp function and ggord plugin for ggplot2 graphics library was used.

Quantitative RT–PCR analysis

Around 1 µg of total RNA was used to synthesize the cDNA library with the QuantiTect Reverse Transcription Kit (Qiagen). Gene-specific primes for qRT–PCR were designed according to the Arabidopsis genome sequence information of TAIR10 (https://www.arabidopsis.org/) and Primer-BLAST (http://www.ncbi.nlm.nih.gov/tools/primer-blast/). Additionally, primer quality was controlled using PCR Primer Stats (http://www.bioinformatics.org/sms2/pcr_primer_stats.html). Primers were ordered from Invitrogen and are listed in Supplementary Table S5. For the PCR procedure, 15 µl reactions were carried out, containing 6 µl of 20× diluted cDNA, 7.5 µl of SYBR Green Supermix (KAPA Biosystems), 0.3 µl of forward primers, 0.3 µl of reverse primers and 0.9 µl of RNase-free H_2O. The reactions were conducted in 384-well plates in RT–PCR systems (Bio-Rad). The standard protocol was set as: 3 min at 95°C, followed by 44 cycles of 3 s at 95°C, 25 s at 60°C and then 5 s at 65°C. Two reference genes, *SAND* (*At2g28390*) and *PDF2* (*At1g13320*), were used, and melt curves were used to check for unique PCR fragments. Reactions were performed in three technical replicates and three biological replicates. Relative transcript levels were calculated with the 2-ΔΔCT method by the Bio-Rad software (Livak and Schmittgen 2001).

Small RNA extraction and quantification

Small RNA was extracted using the innuPREP Micro RNA Kit (Analytik Jena), followed by a quantification using the Small RNA Analysis Kit in Agilent 2100 Bioanalyzer (Agilent), according to the manual instructions.

S-Adenosylmethionine determination

The SAM level was determined with the Bridge-It® S-Adenosyl Methionine Fluorescence Assay Kit (Mediomics), following the manufacturer's instruction. Briefly, 0.3 g of frozen ground root samples was shaken in soluble protein extraction buffer at 4°C for 30 min, before spinning at 12,000 r.p.m. for 10 min. A 30 µl aliquot of the supernatant was transferred to 30 µl of CM Buffer (included in the kit) and incubated at 24°C for 1 h. The suspension was centrifuged at 10,000×*g* at 4°C for 5 min, and the supernatant was collected to measure the fluorescence. The excitation and emission absorbance were 485 and 655 nm, respectively.

Statistical analysis

Data analysis, graphs and statistics were done using R (https://www.r-project.org/). The significance of differences of means for individual traits in this study were determined by *t*-test. Multiple comparisons were conducted using the Tukey HSD method.

Supplementary Data

Supplementary data are available at PCP online.

Funding

This study was supported by the China Scholarship Council; the Faculty of Agriculture of the University of Hohenheim; the German Research Foundation; and the Ministry for Science, Research and Art of Baden-Wuerttemberg [Az: 7533-30-20/1].

Disclosures

The authors have no conflicts of interest to declare.

Acknowledgments

We thank Dr. Sascha Laubinger (Oldenburg, Germany) for *ddc* and *ros1* mutant seeds, and Emil Vatov for comments on the manuscript. X.C. and U.L. conceived the experiment; X.C., B.S. and J.M. performed the experimental work; X.C., B.S., J.M. and U.L. analyzed data and wrote the paper.

References

Aceituno, F.F., Moseyko, N., Rhee, S.Y. and Gutierrez, R.A. (2008) The rules of gene expression in plants: organ identity and gene body methylation are key factors for regulation of gene expression in *Arabidopsis thaliana*. *BMC Genomics* 9: 438.

Asensi-Fabado, M.A., Amtmann, A. and Perrella, G. (2017) Plant responses to abiotic stress: the chromatin context of transcriptional regulation. *Biochim. Biophys. Acta* 1860: 106–122.

Assuncao, A.G., Herrero, E., Lin, Y.F., Huettel, B., Talukdar, S. and Smaczniak, C. (2010) *Arabidopsis thaliana* transcription factors bZIP19 and bZIP23 regulate the adaptation to zinc deficiency. *Proc. Natl. Acad. Sci. USA* 107: 10296–10301.

Benjamini, Y. and Hochberg, Y. (1995) Controlling the false discovery rate—a practical and powerful approach to multiple testing. *J. R. Stat. Soc. Ser. B* 57: 289–300.

Broadley, M.R., White, P.J., Hammond, J.P., Zelko, I. and Lux, A. (2007) Zinc in plants. *New Phytol.* 173: 677–702.

Cakmak, I., Torun, B., Erenoğlu, B., Öztürk, L., Marschner, H., Kalayci, M., et al. (1998) Morphological and physiological differences in the response of cereals to zinc deficiency. *Euphytica* 100: 349–357.

Cao, X. and Jacobsen, S.E. (2002) Locus-specific control of asymmetric and CpNpG methylation by the DRM and CMT3 methyltransferase genes. *Proc. Natl. Acad. Sci. USA* 99: 16491–16498.

Chan, S.W., Henderson, I.R. and Jacobsen, S.E. (2005) Gardening the genome: DNA methylation in *Arabidopsis thaliana*. *Nat. Rev. Genet.* 6: 351–360.

Chen, X., Yuan, L. and Ludewig, U. (2016) Natural genetic variation of seed micronutrients of *Arabidopsis thaliana* grown in zinc-deficient and zinc-amended soil. *Front. Plant Sci.* 7: 1070.

Cokus, S.J., Feng, S., Zhang, X., Chen, Z., Merriman, B., Haudenschild, C.D., et al. (2008) Shotgun bisulphite sequencing of the *Arabidopsis* genome reveals DNA methylation patterning. *Nature* 452: 215–219.

Dowen, R.H., Pelizzola, M., Schmitz, R.J., Lister, R., Dowen, J.M., Nery, J.R., et al. (2012) Widespread dynamic DNA methylation in response to biotic stress. *Proc. Natl. Acad. Sci. USA* 109: E2183–E2191.

Dubin, M.J., Zhang, P., Meng, D., Remigereau, M.S., Osborne, E.J., Paolo Casale, F., et al. (2015) DNA methylation in *Arabidopsis* has a genetic basis and shows evidence of local adaptation. *Elife.* 4: e05255.

Gong, Z., Morales-Ruiz, T., Ariza, R.R., Roldan-Arjona, T., David, L. and Zhu, J.K. (2002) ROS1, a repressor of transcriptional gene silencing in *Arabidopsis*, encodes a DNA glycosylase/lyase. *Cell* 111: 803–814.

Grotz, N., Fox, T., Connolly, E., Park, W., Guerinot, M.L. and Eide, D. (1998) Identification of a family of zinc transporter genes from *Arabidopsis* that respond to zinc deficiency. *Proc. Natl. Acad. Sci. USA* 95: 7220–7224.

Hagmann, J., Becker, C., Muller, J., Stegle, O., Meyer, R.C., Wang, G., et al. (2015) Century-scale methylome stability in a recently diverged *Arabidopsis thaliana* lineage. *PLoS Genet.* 11: e1004920.

Hansen, K.D., Langmead, B. and Irizarry, R.A. (2012) BSmooth: from whole genome bisulfite sequencing reads to differentially methylated regions. *Genome Biol.* 13: R83.

Huang, X.Y., Chao, D.Y., Koprivova, A., Danku, J., Wirtz, M., Muller, S., et al. (2016) Nuclear localised *MORE SULPHUR ACCUMULATION1* epigenetically regulates sulphur homeostasis in *Arabidopsis thaliana*. *PLoS Genet.* 12: e1006298.

Inagaki, S. and Kakutani, T. (2012) What triggers differential DNA methylation of genes and TEs: contribution of body methylation? *Cold Spring Harb. Symp. Quant. Biol.* 77: 155–160.

Ito, T., Sakai, H. and Meyerowitz, E.M. (2003) Whorl-specific expression of the *SUPERMAN* gene of *Arabidopsis* is mediated by cis elements in the transcribed region. *Curr. Biol.* 13: 1524–1530.

Iwasaki, M. and Paszkowski, J. (2014) Identification of genes preventing transgenerational transmission of stress-induced epigenetic states. *Proc. Natl. Acad. Sci. USA* 111: 8547–8552.

Jacobsen, S.E. and Meyerowitz, E.M. (1997) Hypermethylated *SUPERMAN* epigenetic alleles in *Arabidopsis*. *Science* 277: 1100–1103.

Kou, H.P., Li, Y., Song, X.X., Ou, X.F., Xing, S.C., Ma, J., et al. (2011) Heritable alteration in DNA methylation induced by nitrogen-deficiency stress accompanies enhanced tolerance by progenies to the stress in rice (*Oryza sativa* L.). *J. Plant Physiol.* 168: 1685–1693.

Kramer, U., Talke, I.N. and Hanikenne, M. (2007) Transition metal transport. *FEBS Lett.* 581: 2263–2272.

Krueger, F. and Andrews, S.R. (2011) Bismark: a flexible aligner and methylation caller for Bisulfite-Seq applications. *Bioinformatics* 27: 1571–1572.

Kurihara, Y., Matsui, A., Kawashima, M., Kaminuma, E., Ishida, J., Morosawa, T., et al. (2008) Identification of the candidate genes regulated by RNA-directed DNA methylation in Arabidopsis. *Biochem. Biophys. Res. Commun.* 376: 553–557.

Latzel, V., Zhang, Y., Karlsson Moritz, K., Fischer, M. and Bossdorf, O. (2012) Epigenetic variation in plant responses to defence hormones. *Ann. Bot.* 110: 1423–1428.

Law, J.A. and Jacobsen, S.E. (2010) Establishing, maintaining and modifying DNA methylation patterns in plants and animals. *Nat. Rev. Genet.* 11: 204–220.

Le, T.N., Schumann, U., Smith, N.A., Tiwari, S., Au, P.C., Zhu, Q.H., et al. (2014) DNA demethylases target promoter transposable elements to positively regulate stress responsive genes in *Arabidopsis*. *Genome Biol.* 15: 458.

Lev Maor, G., Yearim, A. and Ast, G. (2015) The alternative role of DNA methylation in splicing regulation. *Trends Genet.* 31: 274–280.

Li, H., Handsaker, B., Wysoker, A., Fennell, T., Ruan, J., Homer, N., et al. (2009) The sequence alignment/map format and SAMtools. *Bioinformatics* 25: 2078–2079.

Lin, Y.-F., Liang, H.-M., Yang, S.-Y., Boch, A., Clemens, S., Chen, C.-C., et al. (2009) *Arabidopsis* IRT3 is a zinc-regulated and plasma membrane localized zinc/iron transporter. *New Phytol.* 182: 392–404.

Lister, R., O'Malley, R.C., Tonti-Filippini, J., Gregory, B.D., Berry, C.C., Millar, A.H., et al. (2008) Highly integrated single-base resolution maps of the epigenome in *Arabidopsis*. *Cell* 133: 523–536.

Livak, K.J. and Schmittgen, T.D. (2001) Analysis of relative gene expression data using real-time quantitative PCR and the 2(-Delta Delta C(T)) Method. *Methods* 25: 402–408.

O'Malley, R.C., Huang, S.S.C., Song, L., Lewsey, M.G., Bartlett, A., Nery, J.R., et al. (2016) Cistrome and epicistrome features shape the regulatory DNA landscape. *Cell* 165: 1280–1292.

Probst, A.V. and Mittelsten Scheid, O. (2015) Stress-induced structural changes in plant chromatin. *Curr. Opin. Plant Biol.* 27: 8–16.

Quinlan, A.R. and Hall, I.M. (2010) BEDTools: a flexible suite of utilities for comparing genomic features. *Bioinformatics* 26: 841–842.

Ritchie, M.E., Phipson, B., Wu, D., Hu, Y., Law, C.W., Shi, W., et al. (2015) limma powers differential expression analyses for RNA-sequencing and microarray studies. *Nucleic Acids Res.* 43: e47.

Secco, D., Wang, C., Shou, H., Schultz, M.D., Chiarenza, S., Nussaume, L., et al. (2015) Stress induced gene expression drives transient DNA methylation changes at adjacent repetitive elements. *eLife* 4: e09343.

Secco, D., Whelan, J., Rouached, H. and Lister, R. (2017) Nutrient stress-induced chromatin changes in plants. *Curr. Opin. Plant Biol.* 39: 1–7.

Sharif, R., Thomas, P., Zalewski, P. and Fenech, M. (2012) The role of zinc in genomic stability. *Mutat. Res.* 733: 111–121.

Soppe, W.J., Jacobsen, S.E., Alonso-Blanco, C., Jackson, J.P., Kakutani, T., Koornneef, M., et al. (2000) The late flowering phenotype of *fwa* mutants is caused by gain-of-function epigenetic alleles of a homeodomain gene. *Mol. Cell.* 6: 791–802.

Stroud, H., Greenberg, M.V., Feng, S., Bernatavichute, Y.V. and Jacobsen, S.E. (2013) Comprehensive analysis of silencing mutants reveals complex regulation of the *Arabidopsis* methylome. *Cell* 152: 352–364.

Talukdar, S. and Aarts, M.G. (2008) *Arabidopsis thaliana* and *Thlaspi caerulescens* respond comparably to low zinc supply. *Plant Soil* 306: 85–94.

Teixeira, F.K. and Colot, V. (2009) Gene body DNA methylation in plants: a means to an end or an end to a means? *EMBO J.* 28: 997–998.

van de Mortel, J.E., Almar Villanueva, L., Schat, H., Kwekkeboom, J., Coughlan, S., Moerland, P.D., et al. (2006) Large expression differences in genes for iron and zinc homeostasis, stress response, and lignin biosynthesis distinguish roots of *Arabidopsis thaliana* and the related metal hyperaccumulator *Thlaspi caerulescens*. *Plant Physiol.* 142: 1127–1147.

Yong-Villalobos, L., Cervantes-Pérez, S.A., Gutiérrez-Alanis, D., Gonzáles-Morales, S., Martínez, O. and Herrera-Estrella, L. (2016) Phosphate starvation induces DNA methylation in the vicinity of cis-acting elements

known to regulate the expression of phosphate-responsive genes. *Plant Signal. Behav*. 11: e1173300.

Yong-Villalobos, L., González-Morales, S.I., Wrobel, K., Gutiérrez-Alanis, D., Cervantes-Peréz, S.A., Hayano-Kanashiro, C., et al. (2015) Methylome analysis reveals an important role for epigenetic changes in the regulation of the *Arabidopsis* response to phosphate starvation. *Proc. Natl. Acad. Sci. USA* 112: E7293–E7302.

Zargar, S.M., Fujiwara, M., Inaba, S., Kobayashi, M., Kurata, R., Ogata, Y., et al. (2015) Correlation analysis of proteins responsive to Zn, Mn, or Fe deficiency in *Arabidopsis* roots based on iTRAQ analysis. *Plant Cell Rep.* 34: 157–166.

Zhang, X., Yazaki, J., Sundaresan, A., Cokus, S., Chan, S.W., Chen, H., et al. (2006) Genome-wide high-resolution mapping and functional analysis of DNA methylation in *Arabidopsis*. *Cell* 126: 1189–1201.

Zilberman, D., Gehring, M., Tran, R.K., Ballinger, T. and Henikoff, S. (2007) Genome-wide analysis of *Arabidopsis thaliana* DNA methylation uncovers an interdependence between methylation and transcription. *Nat. Genet*.39: 61–69.